

Thermodynamics of $\text{YBa}_2\text{Cu}_3\text{O}_{6+2x}$: Predictions of the asymmetric next-nearest-neighbor Ising model versus experimental data

R. Tétot, V. Pagot, and C. Picard

Laboratoire d'Étude des Matériaux Hors Équilibre (LEMHE), Université de Paris-Sud, Bâtiment 415, 91405 Orsay Cedex, France

(Received 4 February 1998; revised manuscript received 18 August 1998)

In an earlier paper [Phys. Rev. B **48**, 10 090 (1993)], large discrepancies between the predictions of the two-dimensional asymmetric next-nearest-neighbor Ising (ASYNNNI) model and experimental free enthalpy and enthalpy of oxygen in $\text{YBa}_2\text{Cu}_3\text{O}_{6+2x}$ have been pointed out. In a first step, further experiments have been carried out with particular attention on improving the purity of the samples. Although some differences could be observed between the two sets of measurements, the discrepancies with regard to the model remained. Then, in order to improve the agreement, the ASYNNNI model has been modified in two ways: (i) following Schleger *et al.* [Phys. Rev. B **49**, 514 (1994)], the electron spin and charge degrees of freedom have been included in a pure entropic fashion, (ii) several energies for the oxygen sites have been considered according to the valence states of the neighbor copper ions. We show by using the four- and five-point approximation of the cluster-variation method that these modifications of the ASYNNNI model lead to a satisfactory agreement with experimental thermodynamic functions as well as with the phase diagram. [S0163-1829(99)12521-9]

I. INTRODUCTION

It is well established that the oxygen nonstoichiometry in $\text{YBa}_2\text{Cu}_3\text{O}_{6+2x}$ is largely accommodated by the basal (or chain) plane CuO_x , where x varies from 0 to 0.5. Above the room temperature, the phase diagram comprises three phases: the disordered tetragonal phase (T) stable at high temperature and low oxygen content, and two ordered orthorhombic phases. The first one (O_I), perfect at $x=0.5$, is formed of Cu-O chains along the \mathbf{b} axis. The second one (O_{II}), centered on $x=0.25$, has a structure derived from that of O_I by removing the oxygen in one chain out of two. Basically, this phase diagram has been successfully predicted by the two-dimensional asymmetric next-nearest-neighbor Ising (ASYNNNI) model with three effective pair interactions (EPI's) proposed by de Fontaine *et al.*¹ A recent review on the applicability of this model to $\text{YBa}_2\text{Cu}_3\text{O}_{6+2x}$ may be found in Liu *et al.*² On the other hand, in a previous paper,³ we compared the predictions of the ASYNNNI model with experimental $\Delta G(\text{O}_2)$ and $\Delta H(\text{O}_2)$, respectively, the relative partial molar free enthalpy and enthalpy of oxygen, measured at 873 K as functions of the composition.⁴ At this temperature, only the T and O_I phases are present. Large discrepancies have been observed whatever the set of EPI's used. Principally, the disagreements concerned the variations of $\Delta G(\text{O}_2)$ with composition in the O_I phase and the shape of $\Delta H(\text{O}_2)$ in the neighborhood of the T - O_I transition. In this context, experiments and/or the model may be questioned. Consequently, further experimental determinations of $\Delta G(\text{O}_2)$ and $\Delta H(\text{O}_2)$ have been carried out, with particular attention on improving experimental conditions. The improvements have been made in two directions:

(i) Samples have been prepared in such a way to drastically reduce the presence of secondary phases and to control the microstructure.

(ii) The experimental device has been transformed by coupling the microcalorimeter with the thermobalance,

which allows one to get a direct measurement of $\Delta H(\text{O}_2)$. All the experimental details may be found in Ref. 5.

The comparison between the two experimental determinations of the partial functions at 873 K is shown in Figs. 1(a) and 1(b). No significant difference is observed in the variations of $\Delta G(\text{O}_2)$. Only a small shift in composition has to be noted. On the contrary, the shape of $\Delta H(\text{O}_2)$ is very different from one experiment to another. The presence of secondary phases is probably the main cause of this behavior which is not still completely understood and is being investigated at the present time. In Fig. 1, are also reported the predictions given by the ASYNNNI model with the EPI's provided by first-principles linear muffin-tin orbital-atomic sphere approximation calculations performed by Sterne and Wille.⁸ Calculations have been made by using Monte Carlo simulations and the cluster variation method (CVM) of Kikuchi⁶ in the four- and five-point cluster approximation.⁷ Apart for the T - O_{II} transition, a point which will be discussed further, the two methods yield very close results and only the CVM results are presented in this paper. As already mentioned, large discrepancies on $\Delta G(\text{O}_2)$ can be noted, especially marked in the O_I phase. The calculated $\Delta H(\text{O}_2)$, which is in deep disagreement with old experimental data, qualitatively agrees with the recent data, the calculated discontinuity being simply too small. No set of EPI's has allowed us to significantly improve the agreement. Moreover, the addition of longer-range interactions has also been ineffective. Such inconsistencies between measured thermodynamic properties and those predicted by the ASYNNNI model have also been pointed out by Pörschke *et al.*⁹ in a study on $\text{ErBa}_2\text{Cu}_3\text{O}_{6+2x}$.

Recently, Schleger *et al.*¹⁰ proposed including in the ASYNNNI model the effects of the electron spin and charge degrees of freedom. These authors argue that the behavior of the charge carriers is better represented by a strongly correlated, narrow band, than a broadband approach. This assumption gives rise to two additional entropic terms due to

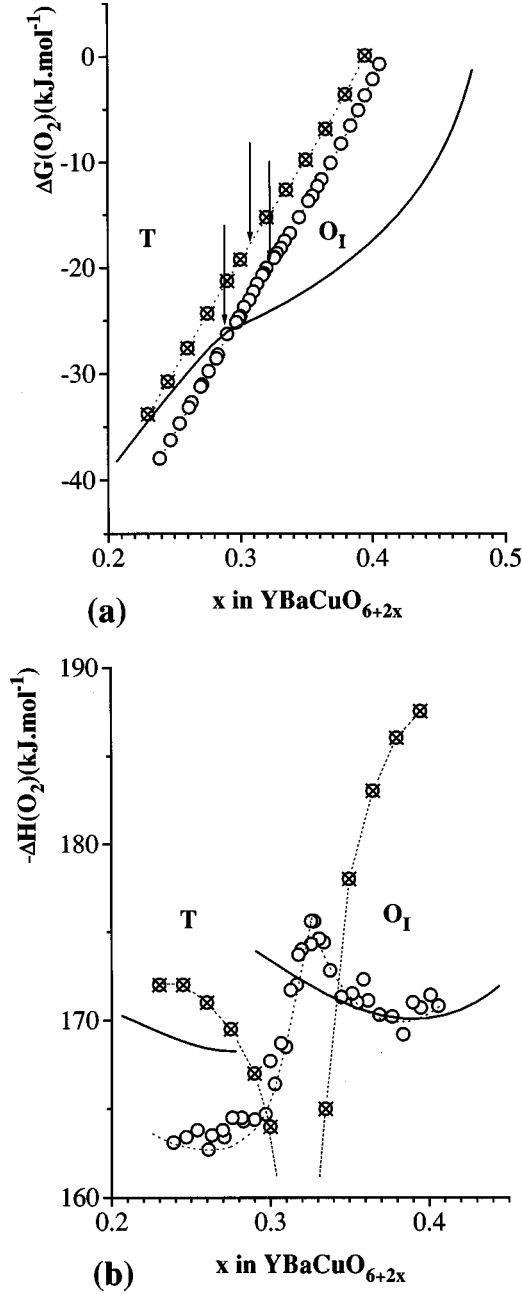


FIG. 1. Plots of $\Delta G(\text{O}_2)$ (a) and $\Delta H(\text{O}_2)$ (b) vs x in $\text{YBa}_2\text{Cu}_3\text{O}_{6+2x}$ at 873 K. Open circles denote recent experiments; cross centered open circles denote previous experiments (lines are just guides for the eyes). Solid lines are the predictions of the basic ASYNNNI model, obtained with the CVM in the four- and five-point cluster approximation and EPI's from Ref. 8. The vertical arrows in (a) show the T - O_I transition compositions.

charge and spin configurational degeneracy. Although their numerical treatment is based on a poor CVM approximation (nearest-neighbor square), the modified model drastically improves the agreement with measured values of the thermodynamic response function, $kT(\partial x/\partial \mu)_T$ (μ is the oxygen chemical potential).

In this paper, we exploit the ideas developed by Schleger *et al.*¹⁰ and, in addition, we consider several energies for the oxygen sites, depending on the valence states of the neighboring copper ions. We show, by using the four- and five-point CVM approximation, that the modifications made to

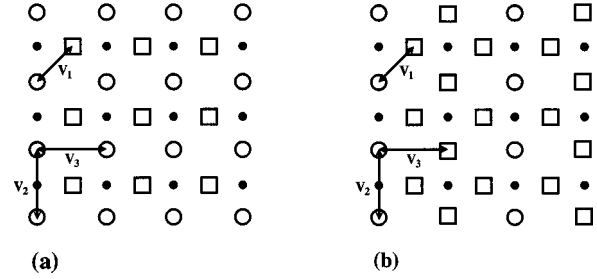


FIG. 2. Schematic representation of the CuO_x basal plane and the three interactions considered in the ASYNNNI model. Big open circles denote oxygen atoms, and open squares oxygen vacancies. Small black circles denote copper atoms. (a) The orthorhombic O_I phase. (b) the orthorhombic O_{II} phase.

the ASYNNNI model lead to a satisfactory agreement with experimental $\Delta G(\text{O}_2)$ and $\Delta H(\text{O}_2)$ as well as with the phase diagram.

II. MODIFICATIONS OF THE ASYNNNI MODEL

The ASYNNNI model is a two-dimensional lattice-gas model aimed at describing the CuO_x basal plane of $\text{YBa}_2\text{Cu}_3\text{O}_{6+2x}$. The oxygen atoms can occupy the sites of a square lattice and interact by three EPI's: V_1 is the nearest-neighbor (NN) interaction, V_2 is the next-nearest-neighbor (NNN) interaction through a Cu atom along the Cu-O chains and V_3 is the NNN interaction perpendicular to the Cu-O chains, as shown in Fig. 2. If the EPI's are $V_1 > 0$, $V_2 < 0$, and $0 < V_3 < V_1$, the two ordered structures O_I and O_{II} are the ground states of the model at the respective concentrations $x = 0.5$ and $x = 0.25$. This model is successful in qualitatively predicting the phase diagram but fails to describe thermodynamic functions such as the oxygen chemical potential. Schleger *et al.*¹⁰ have shown that this can be due to the fact that, in this model, the degrees of freedom of electronic origin are neglected. On the other hand, these effects are contained in defect chemical models (see, for example, Ref. 11) which seems more successful in predicting the chemical potential in a particular range of composition but are unable, on the contrary, to account for the phase diagram. The basic idea of Schleger *et al.*¹⁰ is to introduce the electronic effects in a purely entropic fashion into the ASYNNNI model as described in the following.

It is admitted that an oxygen atom is always surrounded by two Cu^{2+} ions and that a formal Cu^+ ion is surrounded by four oxygen vacancies (see, for example, Refs. 12 and 13). This means that, when an oxygen is added to the basal plane, the number of electron holes may be modified either by changing the formal copper valence or in creating oxygen $2p$ holes. Three processes of absorption of oxygen may then be postulated, depending on the formal valence of the Cu ions NN of the oxygen site, as shown in Fig. 3. At very low oxygen concentration [Fig. 3(a)], the two holes are localized on the two Cu^+ ions NN of the oxygen site. When x increases, the oxygen site may be the NN of a site already occupied and therefore one hole is localized on the available Cu^+ ion and one hole is placed on the O_{2p} orbital [Fig. 3(b)]. Last, if the oxygen site is surrounded by two occupied sites, no Cu^+ is available and the two holes are placed on the O_{2p}

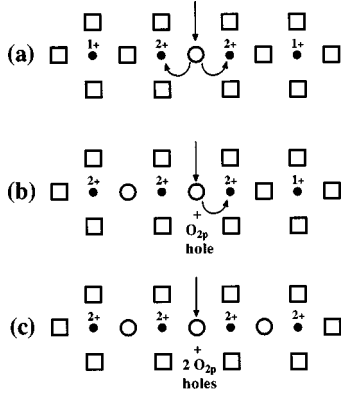
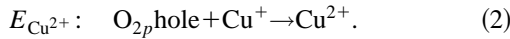
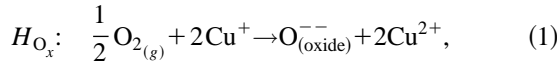


FIG. 3. Schematic description of the various processes for the absorption of an oxygen atom in the basal plane, indicated by the vertical arrows. The symbols are the same as in Fig. 2. 1^+ and 2^+ denote the formal valence of copper ions. (a) The oxygen is isolated and the two holes can go on the NN coppers. (b) There is an oxygen NN and only one copper is available to catch a hole; a O_{2p} hole is created. (c) There are two oxygen atoms that are nearest neighbors and two O_{2p} holes are created.

orbital [Fig. 3(c)]. We have assigned an oxygen site energy for each process. Nevertheless, these energies are not independent and we have chosen to use the energy parameters H_{O_x} and $E_{Cu^{2+}}$ corresponding, respectively, to the following processes:



H_{O_x} is equal to $\frac{1}{2}\Delta H(O_2)$ at an infinite dilution of oxygen ($x \rightarrow 0$) and $E_{Cu^{2+}}$ is the energy difference between a hole in the Cu_{3d} orbital and a hole in the O_{2p} orbital. This energy must be negative. This description gives rise to two additional configurational entropy terms.

The first one, S_c (charge term) comes from the fact that the O_{2p} holes are assumed to hop in an extremely narrow band limit¹⁰ and may be written, assuming a random distribution, as

$$S_c = kN s_{ox} [p_{max} \ln p_{max} - p \ln p - (p_{max} - p) \ln (p_{max} - p)], \quad (3)$$

where $N s_{ox}$ is the number of oxygen sites in the basal plane and p is the number of O_{2p} holes per oxygen site. p_{max} is the number of oxygen sites available for the O_{2p} holes. From experimental arguments (see Ref. 10 and references therein), one can assume a uniform distribution of the O_{2p} holes between the oxygen atoms of the CuO_x and the CuO_2 planes and neglect the apical oxygen atoms. In this way, we obtain $p_{max} = 2 + x$. The charge neutrality condition leads to

$$p = 2x - \langle Cu^{2+} \rangle \quad (4)$$

where $\langle Cu^{2+} \rangle$ is the number of Cu^{2+} ions per oxygen site in the basal plane. On the other hand, we have $\langle Cu^{2+} \rangle + \langle Cu^+ \rangle = \frac{1}{2}$. $\langle Cu^+ \rangle$ can be easily calculated by the CVM: it is equal to the probability of finding the cluster made of four oxygen vacancies surrounding a Cu atom.

The second additional entropy term S_s (spin term) is due to the modification of the number of particles with spin $S = \frac{1}{2}$.¹⁰ In the absence of an O_{2p} hole, this is the total number of Cu^{2+} in the CuO_x and the CuO_2 planes. When a O_{2p} hole is created, it transforms two independent Cu^{2+} into an entity $Cu^{2+} - O_{2p} - Cu^{2+}$ having a spin $S = \frac{1}{2}$. There is a global loss of one spin $S = \frac{1}{2}$. The number of spins $S = \frac{1}{2}$ per oxygen site is therefore $2 + \langle Cu^{2+} \rangle - p$ and the corresponding entropy term is

$$S_s = kN s_{ox} (1 + x - p) \ln 4. \quad (5)$$

These two entropic terms have been added in the CVM free energy functional of the four- and five-point approximations:

$$G_{CVM} = G_{4/5pt} - TS_c - TS_s. \quad (6)$$

III. RESULTS AND DISCUSSION

We present the comparison between experimental and calculated results obtained with the modified ASYNNNI model concerning the thermodynamic functions at 873 K and the phase diagram. The starting EPI's were those of Sterne and Wille⁸ already used in Fig. 1. A satisfactory agreement was obtained with keeping the same ratios $V_2/V_1 = -0.348$ and $V_3/V_1 = 0.16$, with a value $E_{Cu^{2+}}/V_1 = -0.15$, and in fitting the value of $V_1 = 18 \text{ kJ mol}^{-1}$ to the experimental composition of the transition $T-O_I$: $x_I = 0.326$ at 873 K. In order to obtain absolute values for calculations, we have chosen the experimental reference point: $x_I = 0.307$, $\Delta G(O_2) = -23 \text{ kJ mol}^{-1}$ and $\Delta H(O_2) = -165 \text{ kJ mol}^{-1}$ at 873 K.

A. Thermodynamic functions at 873 K

The results concerning $\Delta G(O_2)$ and $\Delta H(O_2)$ at 873 K are plotted in Figs. 4(a) and 4(b). The agreement of $\Delta G(O_2)$ has been drastically improved with respect to Fig. 1, especially regarding the slope breaking between the T and O_I phases. Nevertheless, the calculated mean slope remains slightly too small. For $\Delta H(O_2)$ [Fig. 4(b)], the agreement regarding the discontinuity at the phase transition has also been improved by the modifications of the model. The calculated discontinuity is very sensitive to the value of the energy $E_{Cu^{2+}}$ and increases when $|E_{Cu^{2+}}|$ increases. On the contrary, the global slope of $\Delta G(O_2)$ decreases with increasing $|E_{Cu^{2+}}|$. In a general way, the better the fit of $\Delta G(O_2)$, the worse the fit of $\Delta H(O_2)$ and inversely. Recall that $\Delta H(O_2)$ is very sensitive to experimental conditions whereas $\Delta G(O_2)$ is very stable, as shown in Fig. 1. Consequently it is better to favor a good fit on $\Delta G(O_2)$ than on $\Delta H(O_2)$, while preserving a satisfactory qualitative agreement. From the calculation of $\Delta H(O_2)$ at dilute oxygen concentration, we can estimate the value of the enthalpy of dissolution of an oxygen atom in $YBaCuO_6$ at 873 K: $H_{O_x} = -85.5 \text{ kJ mol}^{-1}$. The uncertainty on this value essentially depends on the choice of the reference point.

B. Phase diagram

Figure 5 compares a few phase diagrams, calculated in the framework of the basic ASYNNNI model, with experimental

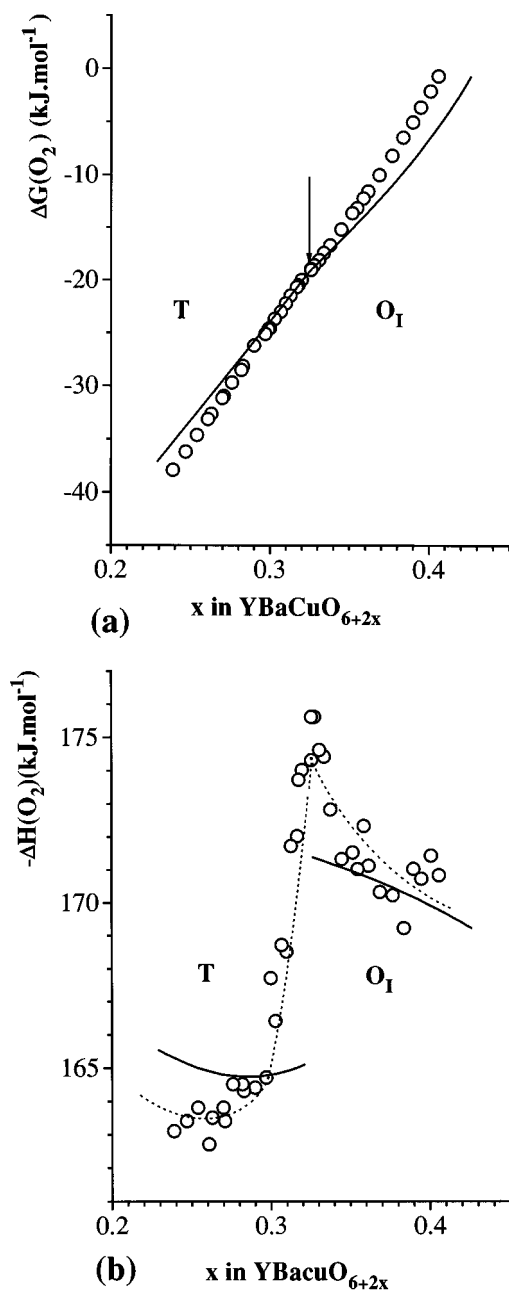


FIG. 4. Plots of $\Delta G(\text{O}_2)$ (a) and $\Delta H(\text{O}_2)$ (b) vs x in $\text{YBa}_2\text{Cu}_3\text{O}_{6+2x}$ at 873 K. Open circles denote experimental data of Ref. 5. The dotted line in (b) is just a guide for the eyes. Solid lines are the predictions of the modified ASYNNNI model, obtained with the CVM in the four- and five-point cluster approximation and parameters reported in the text.

data. Most of these measurements are for the T - O_I transition line and show a great scattering especially for the high temperatures. Nevertheless, it is rather a question of systematic composition shifts than real experimental disagreements. These shifts are probably due to the presence of secondary phases which are very difficult to remove from samples.⁵ In the following, we shall use the results of Picard and Gerdanian (see Ref. 14, and references therein) obtained from Seebeck-effect measurements on samples similar to those used for $\Delta G(\text{O}_2)$ measurements. Two results concern the transition O_I - O_{II} and are in good agreement. Those of Picard and Gerdanian have been obtained from Seebeck-effect mea-

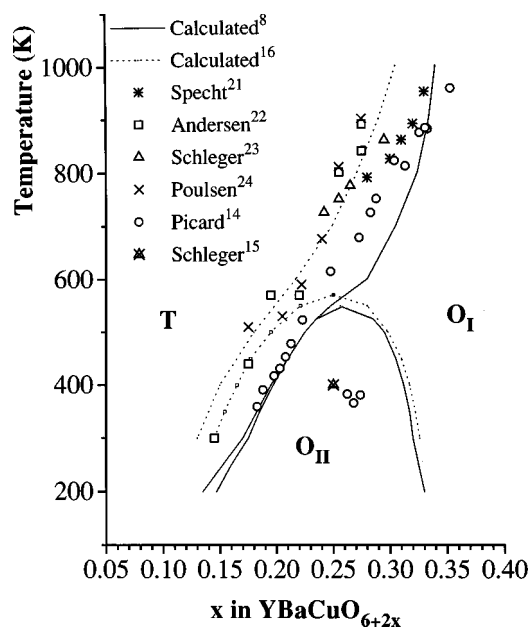


FIG. 5. Comparison between experimental and calculated phase diagrams with the basic ASYNNNI model (Refs. 21–24). (see details in the text). All the initial data, except those of Refs. 14 and 15, are taken from Ref. 16.

surements and that of Schleger *et al.*¹⁵ has been obtained by synchrotron x-ray-diffraction measurements on a single crystal. Solid lines⁸ are calculations using the EPI's of Sterne and Wille used in Fig. 1 and dotted lines are the calculations performed by Hilton *et al.*¹⁶ using EPI's from fits to experimental data. These two calculations are based on the transfer-matrix finite-size-scaling method (TMFSS). We have neglected to represent more recent calculations by Liu *et al.*² from *ab initio* EPI's because the results are rather far from experimental data. All these calculations have some

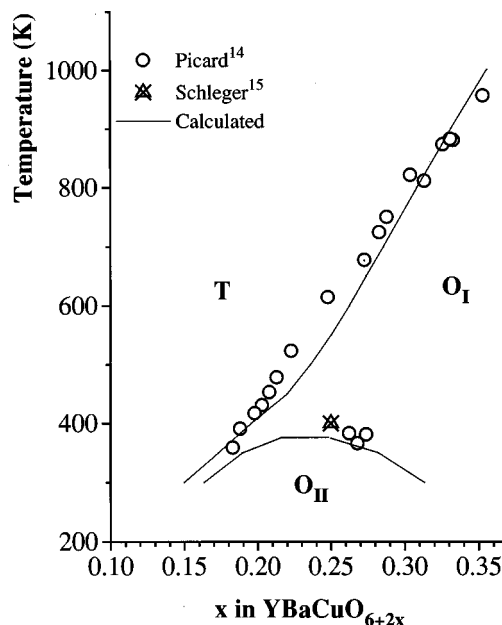


FIG. 6. Comparison between experimental data from Refs. 14 and 15 and the calculated phase diagram with the modified ASYNNNI model.

common features: (i) the slope of the T - O_I transition line at high temperature ($T > 600$ K) is much greater than the experimental one, which leads to a very high order-disorder temperature at $x = 0.5$. (ii) The top of the O_{II} stability region is located much higher than the experimental data.

Figure 6 shows the comparison between the calculated phase diagram with the modified ASYNNNI model and the experimental data of Picard and Gerdanian.¹⁴ Low-temperature calculations have been made by using an algorithm suggested by Finel.¹⁷ It consists of progressively removing the configurations, the probability of which tends towards zero due to the low-temperature effect, and which prevent the convergence of the calculations. It is noteworthy that the agreement has been largely improved, with regard to the prediction of the basic model, regarding the high-temperature domain as well as the O_I - O_{II} transition.

A particular point concerns the fact that, in the framework of the basic ASYNNNI model, all the transitions predicted by the four- and five-point CVM approximation are second order except for the T - O_{II} transition, which is first order (see, for example, Ref. 18). TMFSS calculations,^{16,2} and Monte Carlo simulations¹⁹ do not indicate such first-order transitions. De Fontaine *et al.*¹⁸ have suggested that this problem may be due to an artifact of the four- and five-point approximation of the CVM. In fact, CVM calculations with

larger clusters, up to nine points, still show a two-phase region.²⁰ It is, therefore, an artifact due to the mean-field treatment. Note that Monte Carlo calculations produce the first-order transition by including weak attractive interaction between NNN oxygen chains.²⁰ Our calculations reproduced in Fig. 6 do not show any first-order transitions. Therefore, the modifications provided to the model have removed the artifact of the CVM.

IV. CONCLUSION

The thermodynamic properties of $\text{YBa}_2\text{Cu}_3\text{O}_{6+2x}$, including the oxygen partial functions $\Delta G(\text{O}_2)$ and $\Delta H(\text{O}_2)$ and the phase diagram, have been described in a consistent way by means of a modified ASYNNNI model. The agreement between calculated and experimental results has been drastically improved with regard to the basic model, especially for the oxygen chemical potential and the O_I - O_{II} transition temperature. Some little discrepancies remain, which are probably due to the approximations entering the model, essentially (i) the two dimensionality of the model, (ii) the use of a rigid lattice, (iii) the constant effective pair interactions in the whole composition range, and (iv) the simple way in which the electron holes are treated which leads to a pure ideal entropic contribution.

-
- ¹D. de Fontaine, L. T. Wille, and S. C. Moss, *Phys. Rev. B* **36**, 5709 (1987).
²D. J. Liu, T. L. Einstein, P. A. Sterne, and L. T. Wille, *Phys. Rev. B* **52**, 9784 (1995).
³R. Tétot, C. Giaconia, A. Finel, and G. Boureau, *Phys. Rev. B* **48**, 10 090 (1993).
⁴P. Gerdanian, C. Picard, and J. F. Marucco, *Physica C* **157**, 180 (1989).
⁵V. Pagot, C. Picard, P. Gerdanian, R. Tétot, and C. Legros, *J. Chem. Thermodyn.* **30**, 403 (1998).
⁶R. Kikuchi, *Phys. Rev. B* **81**, 988 (1951).
⁷A. Berera, L. T. Wille, and D. de Fontaine, *J. Stat. Phys.* **50**, 1245 (1988).
⁸P. A. Sterne and L. T. Wille, *Physica C* **162**, 223 (1989).
⁹E. Pörschke, P. Meuffels, and H. Wenzl, *J. Phys. Chem. Solids* **53**, 73 (1992).
¹⁰P. Schleger, W. N. Hardy, and H. Casalta, *Phys. Rev. B* **49**, 514 (1994).
¹¹J. F. Marucco and C. Gledel, *Physica C* **160**, 73 (1989).
¹²J. M. Tranquada, S. M. Heald, A. R. Moodenbaugh, and Y. Xu, *Phys. Rev. B* **38**, 8893 (1988).
¹³J. D. Jorgensen *et al.*, *Phys. Rev. B* **36**, 3608 (1987).
¹⁴C. Picard and P. Gerdanian, *J. Mater. Chem.* **6**, 619 (1996).
¹⁵P. Schleger *et al.*, *Phys. Rev. Lett.* **74**, 1446 (1995).
¹⁶D. K. Hilton, B. M. Gorman, P. A. Rikvold, and M. A. Novotny, *Phys. Rev. B* **46**, 381 (1992).
¹⁷A. Finel (private communication).
¹⁸D. de Fontaine, G. Ceder, and M. Asta, *J. Less-Common Met.* **164-165**, 108 (1990).
¹⁹T. Akrust, M. A. Novotny, P. A. Rikvold, and D. P. Landau, *Phys. Rev. B* **41**, 8772 (1990).
²⁰J. L. Moran-Lopez and J. M. Sanchez, *Physica C* **210**, 401 (1993).
²¹E. D. Specht *et al.*, *Phys. Rev. B* **37**, 7426 (1988).
²²N. H. Andersen, B. Lebech, and H. F. Poulsen, *J. Less-Common Met.* **164/165**, 124 (1990); *Physica C* **172**, 31 (1990); N. H. Andersen (unpublished).
²³P. Schleger, W. N. Hardy, and B. X. Yang, *Physica C* **176**, 261 (1991).
²⁴H. F. Poulsen, N. H. Andersen, and B. Lebech, *Physica C* **173**, 387 (1991).